# Supplementary Materials

## Supplementary Tables

**Table S1** Number of homologous sequences in the multiple sequence alignment

| Name | Structure | Sequence No |
|---|---|---|
| $Na_vAb$ | 3rvy | 3592 |
| $Na_vRh$ | 4dxw | 3857 |
| $Na_vPaS$ | 5x0mA | 1717 |
| | 5x0mB | 3536 |
| | 5x0mC | 3655 |
| | 5x0mD | 3385 |
| | 5x0mAB | 431 |
| | 5x0mAC | 430 |
| | 5x0mAD | 418 |
| | 5x0mBC | 430 |
| | 5x0mBD | 418 |
| | 5x0mCD | 418 |
| $Na_v1.5$ | $Na_v1.5$_DI | 1939 |
| | $Na_v1.5$_DII | 3923 |
| | $Na_v1.5$_DIII | 3390 |
| | $Na_v1.5$_DIV | 3597 |
| | $Na_v1.5$_DI & DII | 430 |
| | $Na_v1.5$_DI & DIII | 429 |
| | $Na_v1.5$_DI & DIV | 428 |
| | $Na_v1.5$_ DII & DIII | 429 |
| | $Na_v1.5$_ DII & DIV | 428 |
| | $Na_v1.5$_ DIII & DIV | 428 |

**Table S2** Binding affinity and binding sites for closed-state LAs and Nav1.5

| Drugs | $K_d$ (μmol/L) | Binding sites | Reference |
|---|---|---|---|
| Pilsicainide | 3209 | - | [1] |
| Bisphenol A | 25.4 ± 1.3 | F1760 | [2] |
| Mexiletine | 6 | - | [3] |

Supplementary Figures

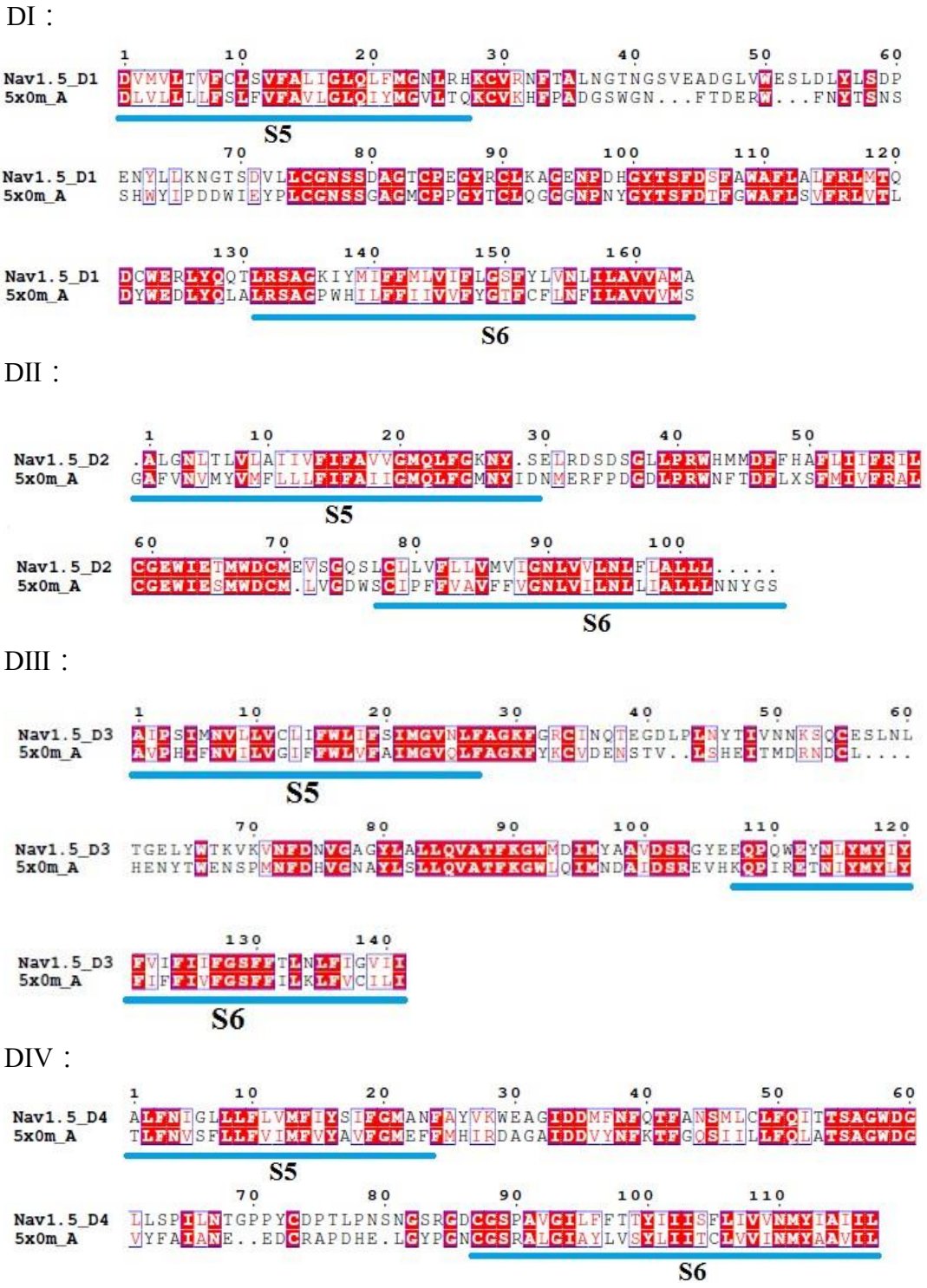


**Fig. S1** Sequence alignments between the domains of $Na_v1.5$ and their templates. S5 and S6 helix in pore domain were shown in blue line at the bottom

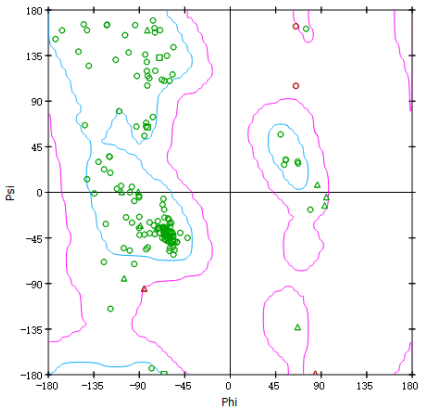


(i) Ramachandran plot for closed state model-0177 (DI)

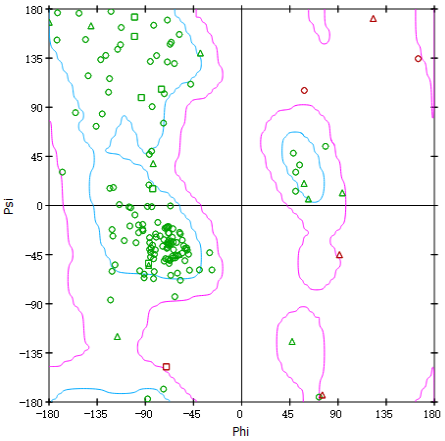


(ii) Ramachandran plot for closed state model-0467 (DI)

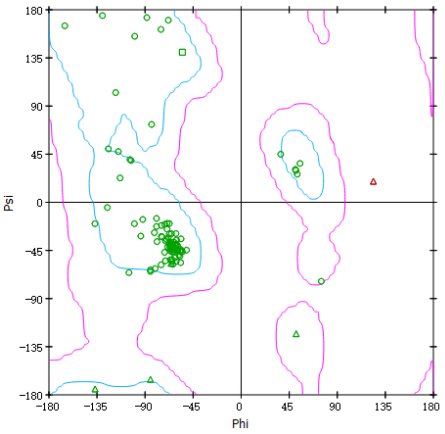


(iii) Ramachandran plot for closed state model-0322 (DII)

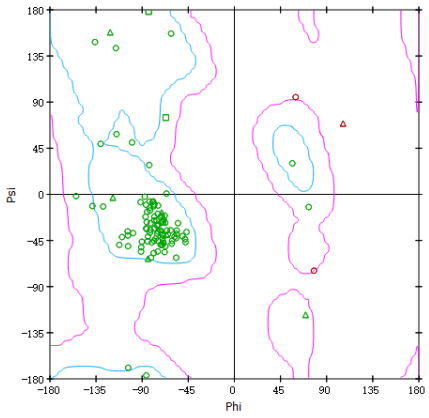


(iv) Ramachandran plot for closed state model-0246 (DII)

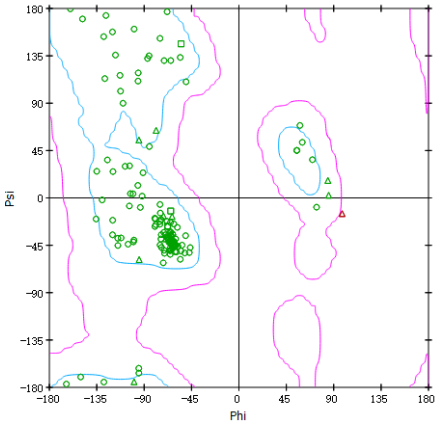


(v) Ramachandran plot for closed state model-0433 (DIII)

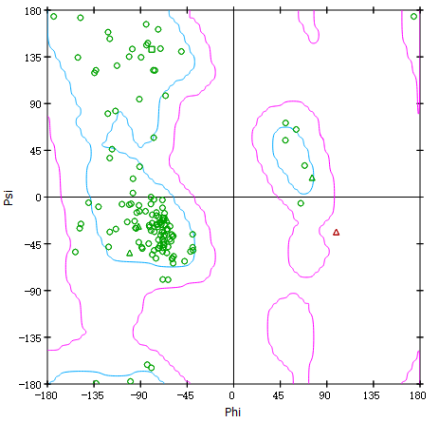


(vi)Ramachandran plot for closed state model-0501 (DIII)

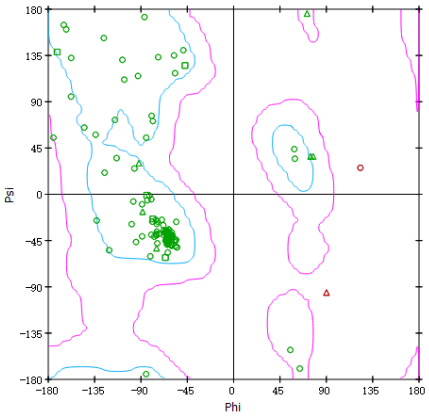


(vii) Ramachandran plot for closed state model-0219 (DIV)

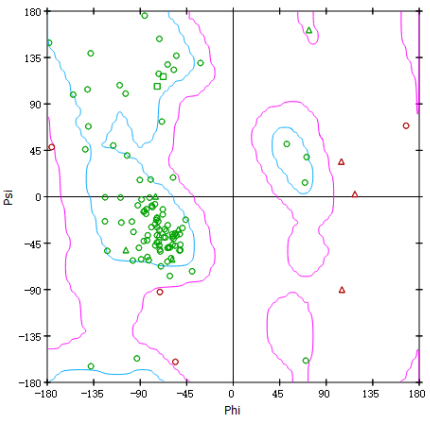


(viii) Ramachandran plot for closed state model-0838 (DIV)

**Fig. S2** Ramachandran plots for selected closed-state segments that formed the PD domain of Nav1.5 (i–viii). (i–ii) models-0177 and 0467 of DI; (iii–iv) models-0322 and 0246 of DII; (v–vi) models-0433 and 0501 of DIII; (vii–viii) models-0219 and 0838 of DIV. Residues are shown with hollow circle except Gly and Pro (they are represented as hollow triangle and square, respectively)

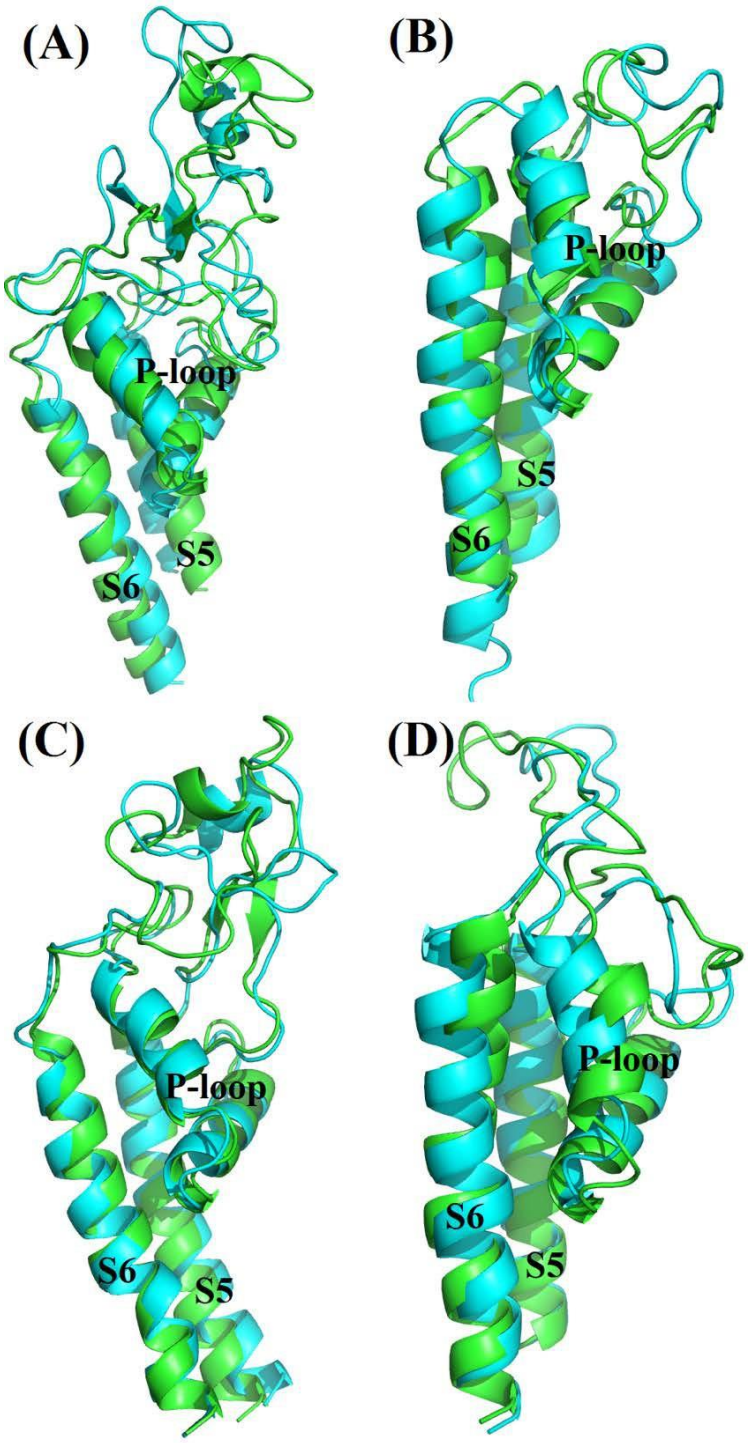


**Fig. S3** Structural alignment of the two selected members for each domain. (**A**) DI: 0177 (green) and 0467 (cyan); (**B**) DII: 0322 (green) and 0980 (cyan); (**C**) DIII: 0433 (green) and 0501 (cyan); (**D**) DIV: 0219 (green) and 0838 (cyan). The mainly differences occur in the regions of P-loop

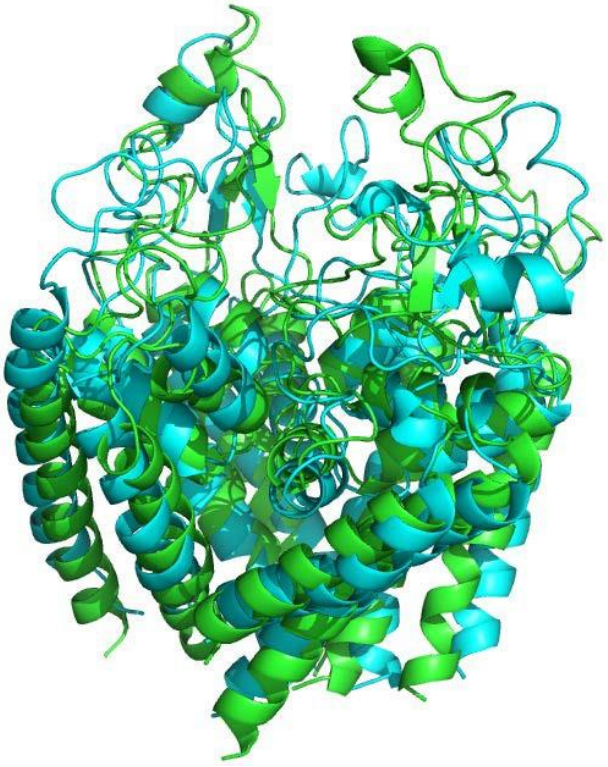

**Fig. S4** Structural alignment between the initial model (cyan) and the model after 300 ns MDsimulation (green)

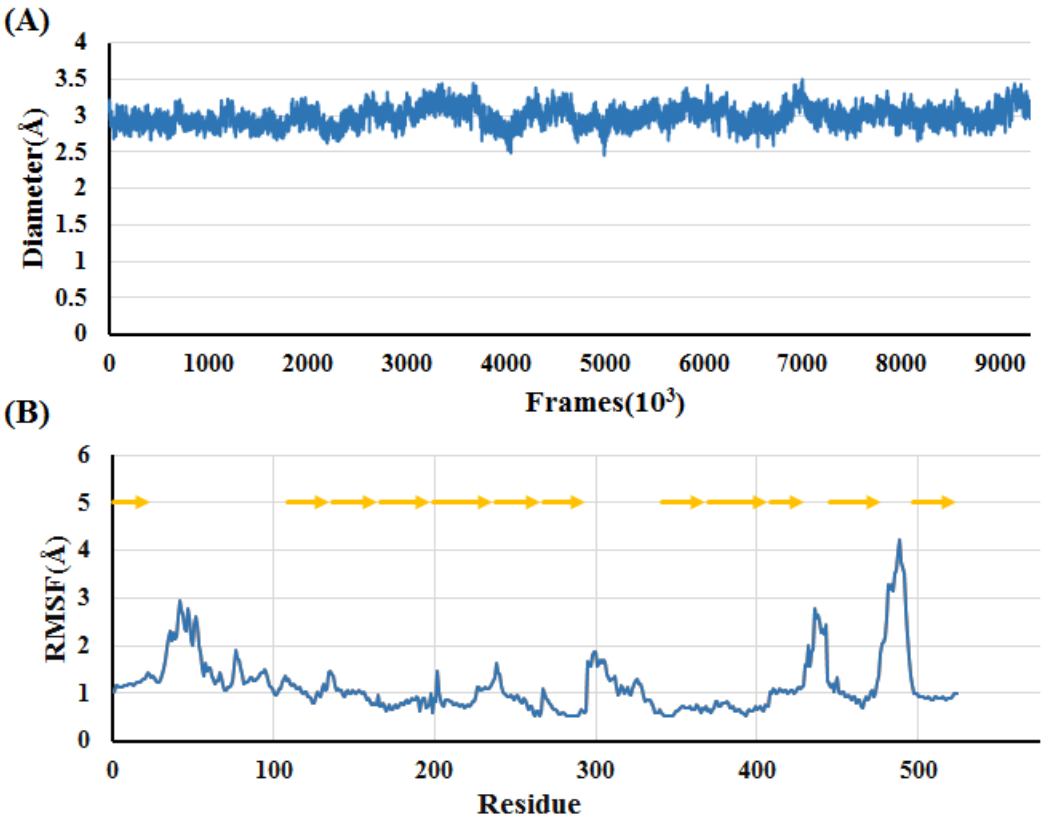


**Fig. S5** The diameter fluctuation of the gate region (**A**) and the RMS analysis of the movements (RMSF) in closed10 (**B**). S5, S6 and P-loops in the four domains of closed10 have been shown at the top of **B** in yellow

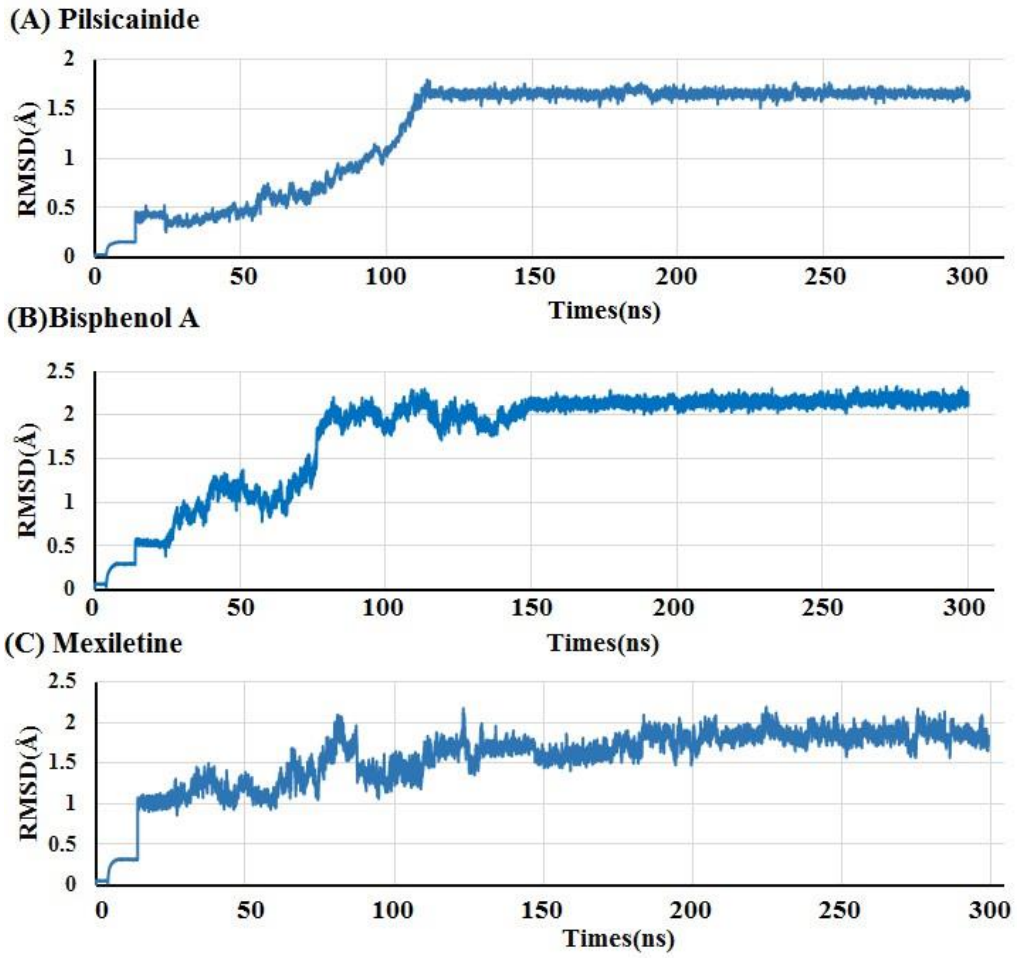


**Fig. S6** Plots of L_RMSD: RMSDs for ligands of $Na_V1.5$_LAs. (**A**) Pilsicainide, (**B**) Bisphenol A and (**C**) Mexiletine

## References:

[1] Desaphy JF *et al.* (2010) Molecular determinants of state-dependent block of voltage-gated sodium channels by pilsicainide. British Journal of Pharmacology, 160(6): 1521–1533

[2] O'Reilly AO *et al.* (2012) Bisphenol A binds to the local anesthetic receptor site to block the human cardiac sodium channel. PLoS One, 7(7): e41667

[3] Moreau A *et al.* (2012) Mexiletine differentially restores the trafficking defects caused by two brugada syndrome mutations. Frontiers in Pharmacology, 3(62): 62